JOURNAL OF GUIDANCE, CONTROL, AND DYNAMICS
Vol. 31, No. 1, January–February 2008

Engineering Notes

ENGINEERING NOTES are short manuscripts describing new developments or important results of a preliminary nature. These Notes should not exceed 2500 words (where a figure or table counts as 200 words). Following informal review by the Editors, they may be published within a few months of the date of receipt. Style requirements are the same as for regular contributions (see inside back cover).

Gyroless Attitude Control of Multibody Satellites Using an Unscented Kalman Filter

James Fisher* and S. R. Vadali†
Texas A&M University, College Station, Texas 77845

DOI: 10.2514/1.30566

Nomenclature

$\mathbf{a}_i$	=	axis of rotation for gimbal i
$\mathbf{C}_x^y$	=	coordinate transformation from frame x to frame y
$\mathbf{F}_{\text{gi}}$	=	force of gravity action on body i
$\mathbf{H}_{xy}$	=	angular momentum vector of body x about point y
$\mathbf{I}_x$	=	inertia tensor of body x
$\mathbf{p}_x$	=	translational momentum vector of body x
$\mathbf{r}_{xy}$	=	vector from point y to point x
$\mathbf{T}_{di}$	=	disturbance torque on body i ($\mathbf{T}_d$ represents the sum over all bodies)
$\mathbf{T}_{ggi}$	=	gravity gradient torque on body i ($\mathbf{T}_{\text{gg}}$ represents the total for all bodies)
$\mathbf{T}_{mi}$	=	control torque on body i
$\mathbf{v}_x$	=	inertial velocity of point x
$\dot{\mathbf{x}}$	=	time derivative of terms in $\mathbf{x}$ in the localized frame
θ_i	=	rotational angle of ith gimbal
$\mathbf{\Omega}$	=	vector of reaction wheel speeds
$\boldsymbol{\omega}_x$	=	angular velocity vector of coordinate frame x with respect to the inertial frame
$\boldsymbol{\omega}_{xy}$	=	angular velocity vector of coordinate frame x with respect to frame y

I. Introduction

THE problem of controlling a multibody spacecraft that must maintain pointing requirements for each of its bodies is addressed. The spacecraft model considered in this Note consists of a main body, a solar panel connected by a two-axis gimbal system, and a three-axis reaction wheel control system. The main body of the satellite is required to maintain a specific orientation with respect to the local-vertical/local-horizontal (LVLH) frame of the body. The solar panel is required to maintain sun-pointing throughout the operation of the spacecraft. Control of the main body orientation is accomplished primarily by reaction wheels. The solar panel pointing requirement is achieved primarily through the use of the two-axis gimbal system. Use of feedback linearization and Lyapunov's direct method allows the synthesis of a simple nonlinear control law, ensuring that tracking accuracy is maintained for each body [1,2]. The implementation of this control requires knowledge of the states of the system. The spacecraft model is assumed to have star trackers as sensors for attitude measurement and angle encoders for measurement of the gimbal angles and rates. The implementation of the feedback control clearly requires a state-estimation technique, not only to smooth the star-tracker measurements, but also to determine the angular velocity of the main body.

State estimation for gyroless spacecraft has received much attention recently [3–6]. This research is motivated by several factors. Failure or degradation of gyros during a flight can result in the loss of a spacecraft or the cancellation of an important mission. Rate gyros may also be too expensive for some spacecraft designs. Improvements in star-tracker accuracy and the rate of data acquisition have made it possible to begin using these as a means to obtain the angular velocity of the spacecraft. This is generally accomplished by use of some form of a Kalman filter [4,7–9]. Most of the research on spacecraft attitude estimation also deals with the estimation of angular velocities of single-body spacecraft. For these cases, it is not difficult to obtain the partial derivatives necessary for the linearization approach of the extended Kalman filter (EKF). The problem of a multibody spacecraft is more difficult. Although the EKF is able to estimate states if the system is linearized, it will be more sensitive to stronger nonlinearities in the system.

Using the unscented Kalman filter (UKF) eliminates the need to take the partial derivatives necessary for the linearization approach of the extended Kalman filter [10–12]. The unscented filter uses a set of sample points, sometimes called sigma points, to map the probability distribution more accurately than the linearized mapping used by the EKF. This filter will be used to obtain the state estimates required by the full-state feedback control used to accurately orient the spacecraft.

This Note is divided as follows. First, the development of the equations of motion for the multibody satellite is outlined in Sec. III. These equations are put into a form that is compatible with the theory behind the UKF, as well as with the control design methodology. The development of the control strategy is discussed next. Immediately following is the presentation of the unscented Kalman filter implementation in Sec. IV. Also in this section, an algorithm for the implementation of the filter is presented. Section V presents the simulated response of the dynamic system under the combined control law and state estimator. A motivating example comparing the responses of the EKF and UKF is presented for the attitude and angular velocity estimation of the main body of the spacecraft. Furthermore, the performance of the UKF will be demonstrated when the attitude, angular velocity, gimbal rates, and gimbal angles are to be estimated.

II. Equations of Motion

The spacecraft model considered is composed of two rigid bodies. The first body (hub) must be pointed accurately throughout the orbit of the satellite. The second body is a panel that must face the sun at all times to provide power to the satellite. These pointing objectives must be satisfied simultaneously. The mass and inertia properties of these bodies are of equivalent orders of magnitude, meaning that the effects of the moving solar panel cannot be treated as a small disturbance. Furthermore, unlike the satellite studied in Agrawal and

Presented as Paper 6163 at the AIAA/AAS Astrodynamics Specialist Conference and Exhibit, Keystone, CO, 21–24 August 2006; received 20 February 2007; revision received 17 July 2007; accepted for publication 20 July 2007.

*Graduate Student, Department of Aerospace Engineering; fisher.james.r@gmail.com. Student Member AIAA.

†Stewart & Stevenson-I Professor, Department of Aerospace Engineering; svadali@aero.tamu.edu. Associate Fellow AIAA.

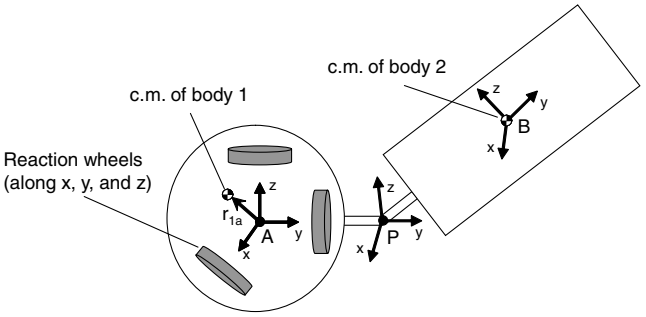

Fig. 1 Simplified diagram of the spacecraft.

Palermo [7], the center of mass of the spacecraft relative to the geometric center of the hub is constantly in motion, due to the movement of the solar panel. The result is that the expressions for the rotational dynamics of the spacecraft also include translational dynamics terms. Figure 1 displays a simplified diagram of the spacecraft. The bodies are connected at point P through a two-axis gimbal mechanism. Point A is an arbitrary point of reference fixed to the hub and it is not necessarily the center of mass of the hub or of the entire spacecraft. The equations of motion are expressed using three coordinate systems. The A-frame, located at A, is fixed to the hub (body 1) and it also serves as a reference coordinate system for many other purposes. The second coordinate system, the P-frame, is located at P and its use is described in the following section. The third coordinate system, the B-frame, is located at point B, the center of mass of the solar panel (body 2).

A. Kinematics

Before we derive the equations of motion of the system, we present the kinematic models for the attitude of the spacecraft. This Note uses Euler parameters to represent the attitude of the hub of the satellite. If the angular velocity of body 1 is given by $\boldsymbol{\omega}_1$, then the differential equation governing the attitude quaternion is given by [13]

$$\dot{\mathbf{q}} = \tfrac{1}{2}\mathbf{B}(\mathbf{q})\boldsymbol{\omega}_1 \tag{1}$$

where

$$\mathbf{B}(\mathbf{q}) = \begin{bmatrix} -q_1 & -q_2 & -q_3 \\ q_0 & -q_3 & q_2 \\ q_3 & q_0 & -q_1 \\ -q_2 & q_1 & q_0 \end{bmatrix} \tag{2}$$

These kinematic equations uniquely determine the attitude of body 1 with respect to the Earth-centered inertial frame (ECI), given its angular velocity and initial attitude. A set of two gimbal angles describes the orientation of the solar panel (body 2) with respect to the hub. The reference frame located at P in Fig. 1 represents the intermediate coordinate axis obtained after the first gimbal rotation with respect to the primary reference frame. This coordinate frame is unique because when expressed in this intermediate frame, the angular velocity of body 2 with respect to body 1 ($\boldsymbol{\omega}_{21}$) is independent of the gimbal-angle values and depends only on their respective rates. Assume that the first gimbal rotation (with magnitude θ_1) is about the y axis of the A-frame (also the same y axis as the P frame) and the second rotation (θ_2) is about the x axis of the P-frame (also the x axis of the B-frame). The orientation of the P-frame with respect to the A-frame and the orientation of the B-frame with respect to the P-frame are given by the following transformations:

$$\mathbf{C}_a^p = \begin{bmatrix} \cos\theta_1 & 0 & -\sin\theta_1 \\ 0 & 1 & 0 \\ \sin\theta_1 & 0 & \cos\theta_1 \end{bmatrix} \qquad \mathbf{C}_p^b = \begin{bmatrix} 1 & 0 & 0 \\ 0 & \cos\theta_2 & \sin\theta_2 \\ 0 & -\sin\theta_2 & \cos\theta_2 \end{bmatrix} \tag{3}$$

The defined gimbal rotations yield the following expression for angular velocity of the second body with respect to the first, expressed in the B-frame:

$$\bar{\mathbf{C}}_p^b \begin{bmatrix} \dot{\theta}_2 \\ \dot{\theta}_1 \end{bmatrix} = \boldsymbol{\omega}_{21} \tag{4}$$

In the preceding expression, $\bar{\mathbf{C}}_p^b$ is a matrix containing the first two columns of $\mathbf{C}_p^b$. The two sets of differential equations presented in this subsection allow for the determination of the attitude of body 1 and body 2, given their respective angular velocities. The angular velocity vectors of the two bodies can be obtained by integrating the dynamic equations of motion.

B. Dynamics

The equations of motion used to model the spacecraft dynamics are derived with respect to point A. Translational and angular momenta of the two bodies are represented by using the notation and derivation of Hughes [14]. The angular momentum of body 1 also includes the contribution due to reaction wheels.

$$\mathbf{p}_1 = m_1(\mathbf{v}_a - \mathbf{r}_{1a} \times \boldsymbol{\omega}_1) \tag{5}$$

$$\mathbf{H}_{1c1} = \bar{\mathbf{I}}_{c1}\boldsymbol{\omega}_1 + \mathbf{I}_w\boldsymbol{\Omega} \tag{6}$$

$$\mathbf{p}_2 = m_2(\mathbf{v}_a - \mathbf{r}_{\mathrm{pa}} \times \boldsymbol{\omega}_1 - \mathbf{r}_{2p} \times (\boldsymbol{\omega}_1 + \boldsymbol{\omega}_{21})) \tag{7}$$

$$\mathbf{H}_{2c2} = \mathbf{I}_{c2}(\boldsymbol{\omega}_1 + \boldsymbol{\omega}_{21}) \tag{8}$$

In the preceding expression, $\mathbf{v}_a$ refers to the inertial velocity of point A and $\mathbf{r}_{1a}$ designates the vector from A to the center of mass of body 1. The angular momentum terms $\mathbf{H}_{1c1}$ and $\mathbf{H}_{2c2}$ refer to the angular momentum of bodies 1 and 2 about their respective centers of mass. The terms $\mathbf{p}_1$ and $\mathbf{p}_2$ refer to the translational momentum of each body. The terms m_1 and m_2 represent the masses of each body. The vector from A to P is denoted by $\mathbf{r}_{\mathrm{pa}}$. Note that $\bar{\mathbf{I}}_{c1}$ designates the moment of inertia of body 1 about its center of mass with the wheels locked. The inertia tensor $\bar{\mathbf{I}}_{c1}$ can be rewritten as $\bar{\mathbf{I}}_{c1} = \mathbf{I}_{c1} + \mathbf{I}_w$, where $\mathbf{I}_w$ is a matrix containing the axial moment of inertia of each wheel along its diagonal. The inertia tensor $\mathbf{I}_{c2}$ is the inertia tensor for body 2, written about its center of mass. In the preceding expression as well as in those that follow, the vector quantities can be expressed in any frame. When implementing the equations of motion in a simulation, it is important to ensure that each expression contains terms in the same frame. The equations are presented here in this form for compactness. The angular and linear momenta of the composite body about A are given by the following:

$$\mathbf{H}_{\mathrm{ta}} = \mathbf{H}_{1c1} + \mathbf{r}_{1a} \times \mathbf{p}_1 + \mathbf{H}_{2c2} + \mathbf{r}_{2a} \times \mathbf{p}_2 \tag{9}$$

$$\mathbf{p}_t = \mathbf{p}_1 + \mathbf{p}_2 \tag{10}$$

The vector $\mathbf{H}_{\mathrm{ta}}$ is the angular momentum of the entire system (body 1 and body 2), $\mathbf{p}_t$ is the translational momentum of the system, and $\mathbf{r}_{2a}$ represents the vector from A to the center of mass of body 2. Proceeding further, equations of motion for the composite body can be written as follows [14]:

$$\dot{\bar{\mathbf{H}}}_{\mathrm{ta}} = -\boldsymbol{\omega}_1 \times \mathbf{H}_{\mathrm{ta}} - \mathbf{v}_a \times \mathbf{p}_t + \mathbf{T}_{\mathrm{gg}} + \mathbf{r}_{\mathrm{ta}} \times \mathbf{F}_g + \mathbf{T}_d - \mathbf{T}_{m1} \tag{11}$$

$$\dot{\mathbf{p}}_t = -\boldsymbol{\omega}_1 \times \mathbf{p}_t + \mathbf{F}_g + \mathbf{F}_d \tag{12}$$

where $\bar{\mathbf{H}}_{\mathrm{ta}} = \mathbf{H}_{\mathrm{ta}} - \mathbf{I}_w(\boldsymbol{\omega}_1 + \boldsymbol{\Omega})$ and $\mathbf{r}_{\mathrm{ta}}$ is the vector from A to the center of mass of the entire system. In the preceding expression, $\dot{\bar{\mathbf{H}}}_{\mathrm{ta}}$ refers to the derivative of $\bar{\mathbf{H}}_{\mathrm{ta}}$ with respect to the A-frame. The reaction wheel equations of motion are written as follows:

$$\mathbf{I}_w(\dot{\boldsymbol{\omega}}_1 + \dot{\boldsymbol{\Omega}}) = \mathbf{T}_{m1} \tag{13}$$

The derivatives in the preceding expression are taken with respect to the A-frame. Finally, to complete the set of equations of motion, we find the angular momentum of the second body about point P:

$$\mathbf{H}_{2p} = \mathbf{H}_{2c2} + \mathbf{r}_{2p} \times \mathbf{p}_2 \tag{14}$$

$$\dot{\mathbf{H}}_{2p} = -(\boldsymbol{\omega}_1 + \boldsymbol{\omega}_{21}) \times \mathbf{H}_{2p} - \mathbf{v}_p \times \mathbf{p}_2 + \mathbf{T}_{gg2} + \mathbf{r}_{2p} \times \mathbf{F}_{g2} + \mathbf{T}'_{m2} + \mathbf{T}_{d2} \tag{15}$$

The velocity of point P is dependent strictly on the velocity at point A and the angular velocity of body 1 through the relationship $\mathbf{v}_p = \mathbf{v}_a - \mathbf{r}_{p1} \times \boldsymbol{\omega}_1$. The vector $\mathbf{T}'_{m2}$ is a vector containing the two solar-panel control torques and a reaction torque. To extract the necessary equations of motion, we can take the dot product of these equations, with the two vectors describing the gimbal-angle rotations. In the actual implementation, the vectors in these equations are expressed in frame B. Taking the dot product of each of these vectors with the equations of motion yields

$$(\bar{\mathbf{C}}_p^b)^T \dot{\mathbf{H}}_{2p} = (\bar{\mathbf{C}}_p^b)^T [-(\boldsymbol{\omega}_1 + \boldsymbol{\omega}_{21}) \times \mathbf{H}_{2p} - \mathbf{v}_p \times \mathbf{p}_2 + \mathbf{T}_{gg2} + \mathbf{r}_{2p} \times \mathbf{F}_{g2} + \mathbf{T}_{d2}] + \mathbf{T}_{m2} \tag{16}$$

In the preceding expression, $\mathbf{T}_{m2} = (\bar{\mathbf{C}}_p^b)^T \mathbf{T}'_{m2}$ and is composed of the two gimbal control torques corresponding to each gimbal axis. Determining the equations of motion in terms of derivatives of the states themselves ($\dot{\boldsymbol{\omega}}_1$, $\dot{\mathbf{v}}_a$, etc.) requires expansion of the derivatives of the various momenta. This task is not trivial and the results are lengthy. As a result, the details are not included here, but can be found in a previous work [15]. By expanding these equations and substituting for $\dot{\mathbf{v}}_a$, we can express the attitude dynamics in the following form:

$$\mathbf{M}(\boldsymbol{\theta})\dot{\mathbf{x}} = \mathbf{f}(\mathbf{x}, \mathbf{q}, \boldsymbol{\theta}, \Gamma) - \mathbf{u} \tag{17}$$

where $\mathbf{M}$ is a matrix that depends on rigid body parameters, as well as on the gimbal angles given by

$$\mathbf{M}(\boldsymbol{\theta}) = \begin{bmatrix} \mathbf{I}_{\text{cm}} & [\mathbf{C}_b^a \mathbf{I}_{2p} + m_2 \mathbf{r}_{\text{tp}}^{\times} (\mathbf{C}_b^a \mathbf{r}_{2p})^{\times}] \bar{\mathbf{C}}_p^b \\ (\bar{\mathbf{C}}_p^b)^T [\mathbf{C}_b^a \mathbf{I}_{2p} + m_2 \mathbf{r}_{\text{tp}}^{\times} (\mathbf{C}_b^a \mathbf{r}_{\text{tp}})^{\times}]^T & (\bar{\mathbf{C}}_p^b)^T \left(I_{2p} + \frac{m_2^2}{m_t} \mathbf{r}_{2p}^{\times} \mathbf{r}_{2p}^{\times} \right) \bar{\mathbf{C}}_p^b \end{bmatrix} \tag{18}$$

where $(\cdot)^{\times}$ is the cross-product matrix, $\mathbf{I}_{\text{cm}}$ is the inertia tensor of the entire system about its center of mass as expressed in the A-frame, $\mathbf{I}_{2p}$ is the inertia of the second body about point P as expressed in the B-frame, and $\mathbf{r}_{\text{tp}}$ is the vector from point P to the c.m. of the entire body. The term $\mathbf{u} = [\mathbf{T}_{m1}, -\mathbf{T}_{m2}]$ is the control torque vector, $\boldsymbol{\theta} = [\theta_2, \theta_1]^T$, $\mathbf{x} = [\omega_1, \dot{\boldsymbol{\theta}}]^T$, and Γ is a vector of states such as $\mathbf{v}_a$ that are not attitude parameters, but appear in the attitude dynamics due to attitude-orbit coupling. Herein it is assumed that the measurements of these additional states are known perfectly.

C. Control Law

The satellite attitude control law is designed using a feedback linearization approach [2]. The stability of this approach can be proven in a Lyapunov framework when all states are known perfectly. A control law that feedback-linearizes the system given in Eq. (17) takes on the following form:

$$\mathbf{u} = \mathbf{f}(\mathbf{x}, \boldsymbol{\theta}, \mathbf{q}, \Gamma) - \mathbf{M}(\boldsymbol{\theta}) \left(\dot{\mathbf{x}}_d - \mathbf{K}_1 (\mathbf{x} - \mathbf{x}_d) - \mathbf{K}_2 \begin{bmatrix} \boldsymbol{\delta\epsilon} \\ \boldsymbol{\theta} - \boldsymbol{\theta}_d \end{bmatrix} \right) \tag{19}$$

In the preceding expression, $(\cdot)_d$ denotes a desired value of a variable. In this manner, $\mathbf{x}_d$ denotes the desired angular velocity of body 1 and the desired gimbal rates (which can be obtained by taking derivatives of the pointing constraint). Although it is not explicitly shown, it is important to realize that $\mathbf{x}_d$ should be expressed in the same frame as $\mathbf{x}$ when the control law is implemented. The control gain matrices $\mathbf{K}_1$ and $\mathbf{K}_2$ are diagonal matrices that can be designed to give desired closed-loop system properties. The term $\boldsymbol{\delta\epsilon}$ (a three-element vector) refers to the last three terms in the error quaternion, which describes the rotation between the actual attitude with respect to LVLH and the desired attitude with respect to LVLH. This is given by [16]

$$\begin{bmatrix} \delta q_0 \\ \boldsymbol{\delta\epsilon} \end{bmatrix} = \begin{bmatrix} q_{d0} & q_{d1} & q_{d2} & q_{d3} \\ -q_{d1} & q_{d0} & q_{d3} & -q_{d2} \\ -q_{d2} & -q_{d3} & q_{d0} & q_{d1} \\ -q_{d3} & q_{d2} & -q_{d1} & q_{d0} \end{bmatrix} \mathbf{q}_{\text{lvlh}} \tag{20}$$

where $\mathbf{q}_{\text{lvlh}}$ is the actual attitude of the spacecraft with respect to the LVLH attitude, and q_{di} represents the ith element of the desired attitude with respect to LVLH. The term δq_0 is the scalar portion of the error quaternion, which, in our notation, is the first term of the quaternion. The evolution of this error quaternion is governed by the following differential equation:

$$\delta \dot{q}_0 = -\tfrac{1}{2} \boldsymbol{\delta\epsilon}^T \boldsymbol{\omega}_e \qquad \boldsymbol{\delta\dot{\epsilon}} = \tfrac{1}{2} (\delta q_0 \boldsymbol{\omega}_e + \boldsymbol{\delta\epsilon} \times \boldsymbol{\omega}_e) \tag{21}$$

If the control law (19) is implemented (assuming that system is known perfectly) then the following closed-loop error dynamics are achieved:

$$\dot{\boldsymbol{\omega}}_e + \mathbf{K}_{1\omega} \boldsymbol{\omega}_e + \mathbf{K}_{2\omega} \boldsymbol{\delta\epsilon} = \mathbf{0}_{3\times 1} \qquad \ddot{\boldsymbol{\theta}}_e + \mathbf{K}_{1\theta} \dot{\boldsymbol{\theta}}_e + \mathbf{K}_{2\theta} \boldsymbol{\theta}_e = \mathbf{0}_{2\times 1} \tag{22}$$

Each of the gain matrices in the preceding equations are taken to be diagonal. The error in the angular velocity of the spacecraft is given by the term $\boldsymbol{\omega}_e = \boldsymbol{\omega}_1 - \boldsymbol{\omega}_d$, and the error in the gimbal angles is given by the vector $\boldsymbol{\theta}_e = \boldsymbol{\theta} - \boldsymbol{\theta}_d$. In the absence of disturbances, the control law results in a decoupled stable response. The gimbal-angle response is given by a second-order dynamic system. Stability of this control law can be proven in a straightforward manner through use of Lyapunov stability theory. For various methods of accomplishing this, see [13]. The control law requires full-state feedback, but the angular velocity of the spacecraft is not measured. As a result, state estimation will be required for successful implementation.

III. Unscented Kalman Filter

This section will describe the implementation of the UKF state-estimation algorithm, the measurement model, the method used in dealing with the quaternion normalization, and how the system dynamics can be put in the proper form for the implementation into the UKF framework. The details of the unscented Kalman filter will not be included here, because s the theory behind the UKF is well known in the literature [10,12,17,18]. The research implementation of the algorithm follows that presented in Crassidis et al. [11], but with a different dynamic model. The UKF uses a dynamic system of the form

$$\mathbf{x}_{k+1}^{(f)} = \mathbf{g}(\mathbf{x}_k^{(f)}, \mathbf{u}_k) \tag{23}$$

with measurements given by

$$\mathbf{y}_k = \mathbf{h}(\mathbf{x}_k^{(f)}) \tag{24}$$

where $\mathbf{x}_k^{(f)}$ denotes the set of states associated with the filter. It is important to note that these are not necessarily the same states associated with the control.

A. State Propagation

Section III provides the information necessary to develop the nonlinear model that will be used to propagate the states estimated by the UKF. This model must be put into a form that is compatible with the UKF; namely, in an expression in the form of Eq. (23). Once the derivatives in Eqs. (11), (12), and (16) are expanded so that they are explicitly dependent on the state variables and their time derivatives, we can couple these with the kinematic relationships in Eqs. (1) and (4) to determine an expression of the form

$$\dot{\mathbf{q}} = \tfrac{1}{2} \mathbf{B}(\mathbf{q}) \boldsymbol{\omega}_1 \tag{25}$$

$$\dot{\boldsymbol{\theta}} = \boldsymbol{\Omega}_g \tag{26}$$

$$\mathbf{M}(\boldsymbol{\theta})\dot{\mathbf{x}} = \mathbf{f}(\mathbf{x}, \mathbf{q}, \boldsymbol{\theta}, \Gamma) - \mathbf{u} \tag{27}$$

The mass matrix in this expression is invertible, and so there are no singularities in the dynamics. The UKF will be used to estimate the vector of filter states given by

$$\mathbf{x}^{(f)} = [\,\mathbf{q}^T \quad \theta_2 \quad \theta_1 \quad \boldsymbol{\omega}_1^T \quad \dot{\theta}_2 \quad \dot{\theta}_1\,]^T \tag{28}$$

where $\boldsymbol{\omega}_1 = [\,\omega_{1x} \quad \omega_{1y} \quad \omega_{1z}\,]^T$. The estimator estimates the components of $\boldsymbol{\omega}_1$ in frame A. By inverting $\mathbf{M}$ in the dynamic equations of motion, we can write the dynamics of the filter states as the following:

$$\dot{\mathbf{x}}^{(f)} = \mathbf{g}(\mathbf{x}^{(f)}, \mathbf{u}) \tag{29}$$

where the $\mathbf{x}^{(f)}$ vector was defined in Eq. (28). The function $\mathbf{g}$ is given by

$$\mathbf{g}(\mathbf{x}^{(f)}, \mathbf{u}) = \begin{bmatrix} \frac{1}{2}\mathbf{B}(\mathbf{q})\boldsymbol{\omega}_1 \\ \boldsymbol{\Omega}_g \\ \mathbf{M}^{-1}(\boldsymbol{\theta})\mathbf{f}(\mathbf{x}, \mathbf{q}, \boldsymbol{\theta}, \Gamma) - \mathbf{M}^{-1}(\boldsymbol{\theta})\mathbf{u} \end{bmatrix} \tag{30}$$

The states in the Γ vector are again assumed to be known perfectly, and therefore are not treated as filter states. In the actual implementation of the filter, these states are propagated between each time step, along with the filter states themselves, to simplify the process. These states, however, are not used in any of the update laws for the filter. This expression can be put into the form of Eq. (23) by numerically integrating the preceding expression between time steps to form a discrete system.

B. Measurement Model

The satellite analyzed in this Note does not have gyroscopes to measure the angular velocity of the spacecraft. The measurements available are the spacecraft attitude (from a star tracker), the gimbal angles, and the gimbal rates. The spacecraft attitude measurements will be assumed to be in the form known as the QUEST measurement model [19]:

$$\tilde{\mathbf{b}}_i = \mathbf{A}(\mathbf{q})\mathbf{r}_i + \boldsymbol{\nu}_{qi} \tag{31}$$

where $\mathbf{A}(\mathbf{q})$ is a 3×3 coordinate transformation matrix. The vector $\mathbf{r}$ is a fixed reference vector and the measurement noise associated with the ith noise vector, $\boldsymbol{\nu}_{qi}$, can be approximated as a zero-mean Gaussian process with a noise covariance given by $\mathbf{R}_{qi} = \sigma_i^2 \mathbf{1}_{3\times 3}$. There may be multiple vector measurements used. For cases in which the gimbal angles and rates are estimated, the gimbal angles and rates are also included as measurements. The gimbal rates and angles are assumed to be of the following form:

$$\tilde{\mathbf{y}}_g = [\,\boldsymbol{\Omega}_g^T \quad \boldsymbol{\theta}^T\,]^T + \boldsymbol{\nu}_g \tag{32}$$

where the $\boldsymbol{\nu}_g$ is zero mean and has a covariance of $\mathbf{R}_g = \mathrm{diag}(\sigma_\Omega^2, \sigma_\Omega^2, \sigma_\theta^2, \sigma_\theta^2)$. When only the attitude and angular velocity of the hub are to be estimated, the measurement vector $\mathbf{y}_k$ is given by

$$\tilde{\mathbf{y}}_k = [\,\tilde{\mathbf{b}}_1^T \quad \cdots \quad \tilde{\mathbf{b}}_m^T\,]^T \tag{33}$$

where m is the number of measurement vectors provided by the attitude sensors. The measurement noise in this case has a covariance of

$$\mathbf{R}_k = \bar{\mathbf{R}}_k = \begin{bmatrix} \mathbf{R}_{q1} & \mathbf{0}_{3\times 3} & \cdots & \mathbf{0}_{3\times 3} \\ \vdots & \ddots & & \vdots \\ \mathbf{0}_{3\times 3} & \cdots & \mathbf{0}_{3\times 3} & \mathbf{R}_{qm} \end{bmatrix} \tag{34}$$

When the filter is required to measure the attitude and angular velocity of the hub, as well as the gimbal angles and rates, the following input vector is used:

$$\tilde{\mathbf{y}}_k = [\,\tilde{\mathbf{b}}_1^T \quad \cdots \quad \tilde{\mathbf{b}}_m^T \quad \tilde{\mathbf{y}}_g^T\,]^T \tag{35}$$

This measurement noise in this case has a covariance of

$$\mathbf{R}_k = \begin{bmatrix} \bar{\mathbf{R}}_k & \mathbf{0}_{3m\times 4} \\ \mathbf{0}_{4\times 3m} & \mathbf{R}_g \end{bmatrix} \tag{36}$$

C. Quaternion Normalization

It is well known that when using a quaternion attitude representation, any updates produced from the estimator can violate the quaternion unit-norm constraint. Although it is still possible to use an additive approach for updating the quaternion [20], it is desirable to update the quaternion in such a way that it is automatically unit norm. This can be accomplished by using the quaternion representation for state propagation, but transforming this to an unconstrained attitude representation for the update, as in Crassidis and Markley [11]. The methodology used in this Note involves the update of an error quaternion. At each time step before an update is performed, the following error quaternion is defined:

$$\boldsymbol{\delta}\mathbf{q}_k^-(i) = \hat{\mathbf{q}}_k^-(i) \otimes [\hat{\mathbf{q}}_k^-(1)]^{-1} \qquad i = 1, \ldots, 2n+1 \tag{37}$$

where $\hat{\mathbf{q}}_k^-(1)$ is the preupdate quaternion estimate (the estimate from the last step). If we represent the quaternion by $\hat{\mathbf{q}}_k^-(i) = [\,\hat{q}_0(i) \quad \hat{\boldsymbol{\rho}}(i)\,]^T$, then the inverse operator is defined as $[\hat{\mathbf{q}}_k^-(1)]^{-1} = [\,\hat{q}_0(1) \quad -\hat{\boldsymbol{\rho}}(1)\,]^T$. The preupdate error quaternion corresponding to $i = 1$ will always be $\boldsymbol{\delta}\mathbf{q}_k^-(1) = [\,1 \quad 0 \quad 0 \quad 0\,]^T$. The rest of the values are errors in rotations with respect to the mean of the distribution. These error quaternions will be used in the update law. The error quaternion is represented as

$$\boldsymbol{\delta}\mathbf{q}_k^-(i) = \begin{bmatrix} (\delta q_0^-)_k(i) \\ \boldsymbol{\delta}\boldsymbol{\rho}_k^-(i) \end{bmatrix} = \begin{bmatrix} \sqrt{1 - [\boldsymbol{\delta}\boldsymbol{\rho}_k^-(i)]^T \boldsymbol{\delta}\boldsymbol{\rho}_k^-(i)} \\ \boldsymbol{\delta}\boldsymbol{\rho}_k^-(i) \end{bmatrix} \tag{38}$$

The error quaternion can now be represented in terms of the three components of $\boldsymbol{\delta}\boldsymbol{\rho}_k^-(i)$. From here, we can redefine the $\boldsymbol{\chi}_k^{(i)}$ term that is used to determine the statistical properties of the propagated distribution. The postupdate estimate of the state vector, $\mathbf{x}_k^{(f)}$, is given by $(\hat{\mathbf{x}}_k^{(f)})^+$, which is defined as

$$(\hat{\mathbf{x}}_k^{(f)})^+ = \boldsymbol{\chi}_k^{(1)} = \begin{bmatrix} \boldsymbol{\delta}\boldsymbol{\rho}_k^+(1) \\ (\hat{\boldsymbol{\omega}}_1)_k^+(1) \\ (\hat{\boldsymbol{\Omega}}_g)_k^+(1) \\ \hat{\boldsymbol{\theta}}_k^+(1) \end{bmatrix} \tag{39}$$

Therefore, the quaternion terms used to propagate the equations of motion must be converted to error quaternions after propagation. From here they can be updated and the sigma points can be added. After the state estimate has been updated using the most recent measurements and the sigma points have been added, the actual attitude quaternion must be determined from the updated error quaternions. This is accomplished by using the definition of the error quaternion:

$$\mathbf{q}_k^+(i) = \boldsymbol{\delta}\mathbf{q}_k^+(i) \otimes \mathbf{q}_k^-(1) \tag{40}$$

From this point, we are back to propagation. In this manner, the quaternion update is performed without violation of the norm constraint. Unfortunately, this is only true when $\|\boldsymbol{\delta}\boldsymbol{\rho}_k^+(i)\| \leq 1$. If this condition is violated, the error quaternion $\boldsymbol{\delta}\mathbf{q}_k^+(i)$ will not be unit norm. This can be satisfied by ensuring that initial covariance estimates are set correctly. It is important that the error in the initial quaternion estimates also be small enough to prevent this from occurring.

D. Filter Algorithm

An overview of the steps required for implementation of the filter will be presented here.

1) Use the initial state covariance matrix to build an initial set of sigma points. For all states except for the attitude quaternion, add these points to the initial estimates of the states. For each set of sigma points, find the associated error quaternion and find the associated attitude quaternion using Eq. (40).

2) Propagate each set of state vectors ($2n + 1$ sets) to the next time step using Eq. (29).

3) Find the error quaternion associated with each sigma point set using Eq. (37). The rest of each $\boldsymbol{\chi}_{k+1}(i)$ can be obtained directly from the propagated states.

4) Find the properties of the propagated distribution ($\mathbf{P}_{k+1}^{-}$ etc.) and update the states and covariance.

5) Build a new set of sigma points for the states. Find the new attitude quaternion associated with each set using Eq. (40). Return to step 2.

IV. Results

Two sets of results are presented in this section. The first set compares the response of the UKF to that of the EKF for the given multibody dynamics, in which the states to be estimated are only attitude and angular velocity. The second set highlights the performance of the UKF itself when it is required to estimate attitude, angular velocity, gimbal rates, and gimbal angles.

A. Motivation for Using UKF over EKF

In this section, we show a situation that can occur when using the EKF for feedback control. For this example, the EKF and UKF are both required to estimate only the inertial attitude and inertial angular velocity of body 1. It is assumed that the gimbal angles and rates are known perfectly. The system is required to maintain sun-pointing during a body-1 LVLH attitude reorientation maneuver from $\mathbf{q} = [1 \quad 0 \quad 0 \quad 0]^T$ to $\mathbf{q} = [0.5 \quad 0.5 \quad 0.5 \quad 0.5]^T$. The measurements for the estimator come from a vector measurement with variance $\sigma_q = 0.0015$. The errors in the estimates for the quaternion and angular velocity of body 1 are shown in Fig. 2. During this reorientation, the gimbal angles must undergo large changes between two extreme values. This introduces a large degree of nonlinearity into the system during these periods of rapid transition. The system moment of inertia undergoes a large change in its off-diagonal values. The principal eigenvalues and eigenvectors also experience large changes. As a result, the EKF is not able to retain accuracy over the course of the simulation. Although this behavior is not observed for every type of maneuver, it is an important case because it displays the strength of the UKF even in the face of large changes in system behavior (as long as these are modeled). The orbit of the spacecraft is elliptic, with angular velocities ranging between 4×10^{-4} and 7×10^{-4} rad/s. The errors experienced by the EKF during the maneuver can be as high as 10% of the actual angular velocity. This type of error leads to chatter and possibly even loss of control of the spacecraft and is therefore unacceptable. This motivates the use of the UKF for the feedback scheme.

B. Full System Response

In this section, we demonstrate the response of the UKF when it is also required to estimate the gimbal angles and rates of the system. The problem of estimation of the gimbal rates and angles presents an added difficulty because many of the inertia terms and distance vectors in Eqs. (11) and (16) depend on them. When the gimbal angles are not being estimated, they can be treated as an input and the linearization used by the EKF is straightforward. Including the gimbal angles in the state vector makes the linearization required by the EKF a very painful process. This could be alleviated with the use of a numerical linearization scheme, but the implementation of this requires n (or more) recalculations of the derivative vector $\mathbf{f}$. In terms of number of computations, this is nearly equivalent to the propagation of half of the sigma points required by the UKF (on the order of n^2) when using a first-order Euler integration. In addition, there is still the propagation of the covariance matrix. The ability of the UKF implementation to perform without requiring linearization makes it an attractive choice for situations such as these. As a result, this section details only the UKF implementation.

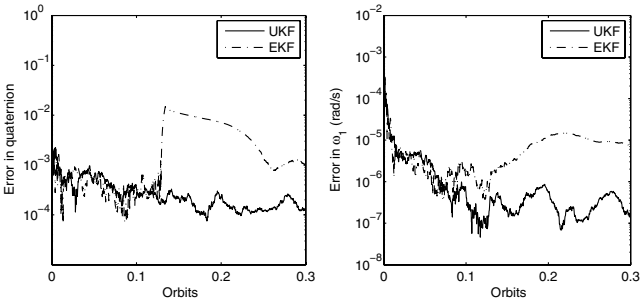

Fig. 2 Error estimates in quaternion and ω_1 for EKF and UKF large gimbal maneuver.

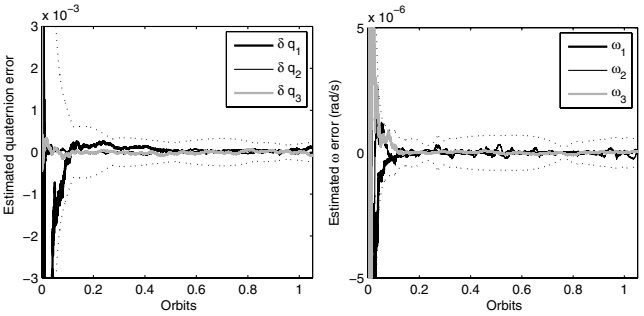

Fig. 3 Error in estimated quaternion and ω_1.

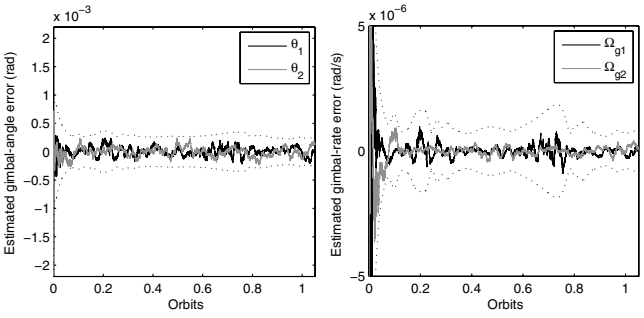

Fig. 4 Error in estimated gimbal angles and gimbal-angle rates.

The state estimator is required to determine the spacecraft attitude, the angular velocity of body 1, the gimbal-angle rates and gimbal angles from measurements of the spacecraft attitude, and gimbal-angle and rate measurements. These are all assumed to be noisy measurements and are assumed to be on the same update frequency. These state estimates will be used to implement a feedback control scheme that is capable of achieving pointing objectives for both bodies.

The following set of figures will display the results of this simulation. Figure 3 shows the error between the real and estimated quaternion, as well as the error between the real and estimated angular velocity of body 1. The $3-\sigma$ bounds in these figures are shown for the smallest of the three variables, to reduce clutter. The values were nearly identical in all the cases tested. The filter convergence occurs within 0.1 orbits. The convergence is not as fast as that observed when the gimbal angles were assumed to be known. This is a result of the addition of more complexity to the filter. Figure 4 shows the error response of the gimbal angles and rates. The accuracy of these values is important because many of the parameters in the feedback control law (such as the inertia tensor) depend upon the gimbal angles. If the estimates of these values are inaccurate, then the control will not be able to converge accurately, due to errors in parameter values.

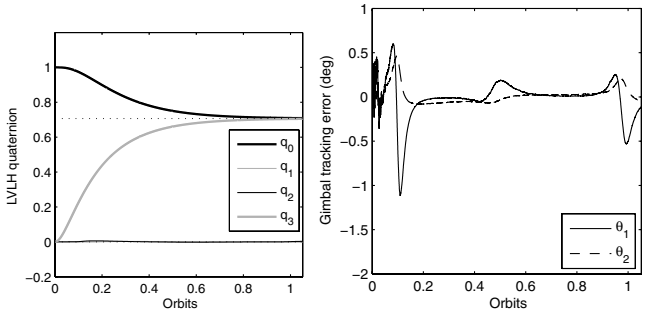

Fig. 5 Body to LVLH quaternion and gimbal-angle tracking error.

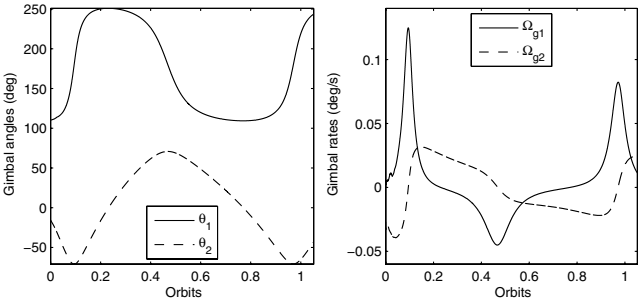

Fig. 6 Gimbal-angle and rate values.

Figure 5 demonstrates the convergence of the control law. The system is given an initial tracking error and is required to maneuver to the desired attitude over the course of one orbit. Figure 5 demonstrates the ability of the control law to achieve accurate tracking even when state feedback information is provided by a state estimator instead of from actual state measurements. The figure depicts the convergence of the hub to the desired LVLH pointing and the tracking error of the gimbal angles with respect to their desired values. The gimbal-angle tracking error is within ± 0.5 deg. Figure 6 shows the gimbal-angle values throughout the maneuver. The gimbal angles are required to vary over a large range throughout an orbit. Figures 5 and 6 show that the tracking error in the gimbal-angle response occurs at points at which the gimbals are required to undergo a large change in value very quickly. This is particularly true

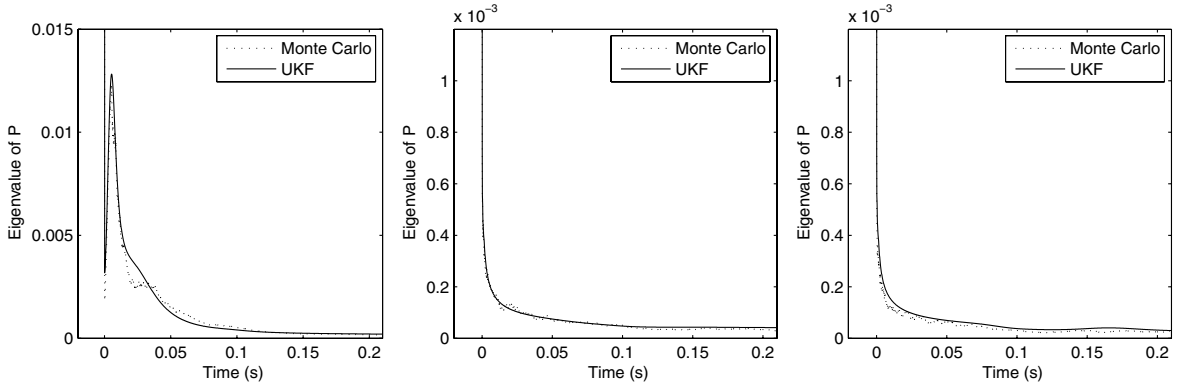

Fig. 7 Comparison of theoretical and Monte Carlo covariance eigenvalues 1–3.

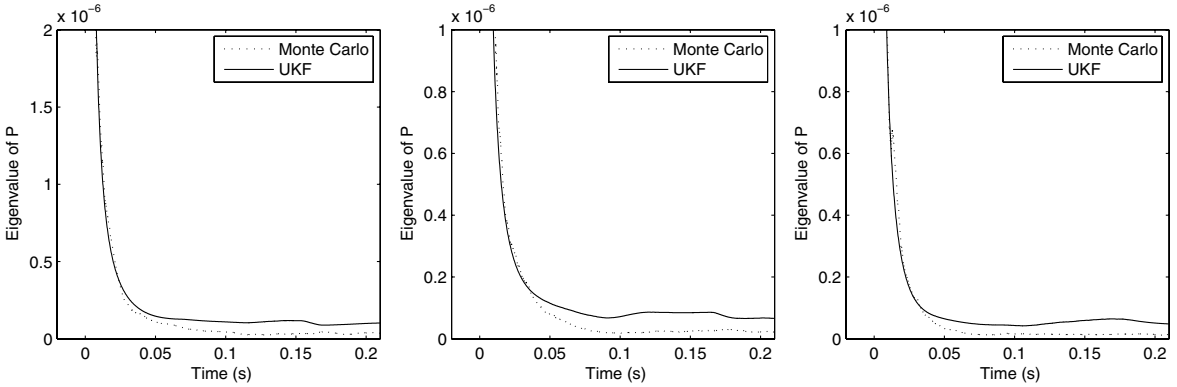

Fig. 8 Comparison of theoretical and Monte Carlo covariance eigenvalues 4–6.

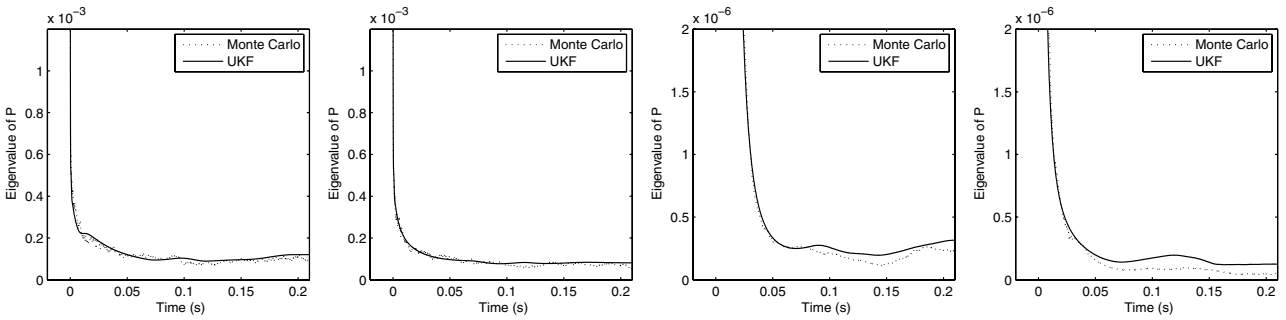

Fig. 9 Comparison of theoretical and Monte Carlo covariance eigenvalues 7–10.

of θ_1. The inertia tensor and the total center of mass vector undergo large changes with respect to θ_1 when the θ_2 gimbal has a larger value. Comparing Figs. 5 and 6 shows that the errors also occur when the θ_2 gimbal attains its maximum and minimum values. This also occurs when the θ_1 gimbal rate is at a maximum. These gimbal-angle and gimbal-rate conditions result in the behavior of the system becoming "more nonlinear." Figure 4 demonstrates that these gimbal-angle and gimbal-rate requirements also have effects on the performance of the UKF. These figures demonstrate the success of the UKF in performing accurate state estimation for a complex nonlinear dynamic system. Furthermore, it demonstrates the ability of the UKF to be successfully used in a feedback control scheme.

To verify that the filter is performing accurately, we consider the covariance matrix as estimated by the filter and the covariance matrix as estimated by Monte Carlo simulation. These matrices should be very close to one another (if the UKF is estimating properly). The Monte Carlo covariance estimates at each time step are obtained by first finding the error between the real and estimated states at each time step t_k. These are then used to find the covariance matrix by using the following:

$$\mathbf{P}_{\text{mc}}(t_k) = \frac{1}{N_{\text{mc}}} \sum_{i=1}^{N_{\text{mc}}} \tilde{\mathbf{x}}(t_k)\tilde{\mathbf{x}}(t_k)^T \tag{41}$$

where $\tilde{\mathbf{x}}$ is the error between the real and estimated states and N_{mc} is the number of simulations used in the Monte Carlo test. Each of these simulations is computed using different random initial conditions. As a comparison of the Monte Carlo and estimated covariances, we look at the eigenvalues of each of these covariance matrices. The eigenvalues of the matrices give some measure of the size of each of the ellipsoids defined by each of the covariance matrices. Although these do not give any orientation information, they can at least help determine if the UKF is accurately representing the size of the covariance ellipsoid. Figures 7–9 show the time evolution of eigenvalues of the covariance matrices. Eigenvalues 1–3 closely correspond to the error quaternion states. The eigenvectors for these values lie almost completely in the space spanned by the error quaternion states. Eigenvalues 4–6 correspond almost exclusively to the angular velocity states, eigenvalues 7–8 correspond to the gimbal-angle states, and eigenvalues 9–10 correspond to the gimbal rates. Although the eigenvalues are not identical, they are within the same order of magnitude in all cases, and their behavior matches relatively well. The theoretical values are conservative, but this is to be expected for numerical simulation. These results show that the filter is performing accurately and that the results obtained are characteristic of the filter behavior.

V. Conclusions

This Note presented the design of a state-estimation and feedback control scheme for a multibody satellite in an elliptic orbit about the Earth. The satellite is composed of two bodies. One body of the satellite must maintain a fixed pointing attitude with respect to the LVLH frame and the other must maintain sun-pointing. The feedback control scheme requires information about each system state, but the satellite does not use gyroscopes for angular velocity measurement. An unscented Kalman filter is used to determine the angular velocity of the primary body for use with the feedback control law, as well as to reduce the noise levels in the signals. An example is presented that demonstrates the ability of the UKF to accurately estimate states in the presence of nonlinearity when the EKF is unable to maintain accuracy. For this reason, the UKF is used to provide state estimates for the nonlinear feedback control. The performance of the unscented filter is analyzed for the case when the attitude of the hub and angular velocities of both the bodies are estimated. The complexity of this problem renders it ideal for the implementation of the UKF because it does not require linearization of the system.

References

[1] Slotine, J.-J. E., and Li, W., *Applied Nonlinear Control*, Prentice–Hall, Englewood Cliffs, NJ, 1991.

[2] Khalil, H. K., *Nonlinear Systems*, 3rd ed., Prentice–Hall, Upper Saddle River, NJ, 1996.

[3] Akella, M. R., Valdivia, A., and Kotamraju, G. R., "Velocity-Free Attitude Controllers Subject to Actuator Magnitude and Rate Saturations," *Journal of Guidance, Control, and Dynamics*, Vol. 28, No. 4, 2005, pp. 659–666.

[4] Tortora, P., Oshman, Y., and Santoni, F., "Spacecraft Angular Rate Estimation from Magnetometer Data Only Using an Analytic Predictor," *Journal of Guidance, Control, and Dynamics*, Vol. 27, No. 3, 2004, pp. 365–373.

[5] Oshman, Y., and Markley, F. L., "Sequential Attitude and Attitude-Rate Estimation Using Integrated-Rate Parameters," *Journal of Guidance, Control, and Dynamics*, Vol. 22, No. 3, 1999, pp. 385–394.

[6] Tsiotras, P., "A Passivity Approach to Attitude Stabilization Using Nonredundant Kinematic Parameterizations," *Proceedings of the 34th IEEE Conference on Decision and Control*, Vol. 1, Inst. of Electrical and Electronics Engineers, Piscataway, NJ, Dec. 1995, pp. 515–520.

[7] Agrawal, B. N., and Palermo, W. J., "Angular Rate Estimation for Gyroless Satellite Attitude Control," AIAA Guidance, Navigation, and Control Conference and Exhibit, Monterey, CA, AIAA Paper 2002-4463, Aug. 2002.

[8] Crassidis, J. L., Markley, F. L., and Cheng, Y., "A Survey of Nonlinear Attitude Filtering Methods," *Journal of Guidance, Control, and Dynamics*, Vol. 30, No. 1, 2007, pp. 12–18. doi:10.2514/1.22452

[9] Psiaki, M. L., "Global Magnetometer-Based Spacecraft Attitude and Rate Estimation," Vol. 27, No. 2, 2004, pp. 240–250.

[10] Julier, S. J., Uhlrnann, J. K., and Durrant-Whyte, H. F., "A New Approach for Filtering Nonlinear Systems," *Proceedings of the American Control Conference*, Vol. 3, Inst. of Electrical and Electronics Engineers, Piscataway, NJ, June 1995, pp. 1628–1632.

[11] Crassidis, J. L., and Markley, F. L., "Unscented Filtering for Spacecraft Attitude Estimation," *Journal of Guidance, Control, and Dynamics*, Vol. 26, No. 4, 2003, pp. 536–542.

[12] Wan, E. A., and van der Merwe, R., "The Unscented Kalman Filter for Nonlinear Estimation," *Proceedings of the IEEE 2000 Adaptive Systems for Signal Processing, Communications, and Control Symposium*, Inst. of Electrical and Electronics Engineers, Piscataway, NJ, Oct. 2000, pp. 153–158.

[13] Schaub, H., and Junkins, J. L., *Analytical Mechanics of Space Systems*, AIAA, Reston, VA, 2003.

[14] Hughes, P. C., *Spacecraft Attitude Dynamics*, Wiley, New York, 1986.

[15] Fisher, J., and Vadali, S. R., "Gyroless Attitude Control of Multi-Body Satellites Using an Unscented Kalman Filter," AIAA/AAS Astrodynamics Specialist Conference and Exhibit, Keystone, CO, AIAA Paper 2006-6163, Aug. 2006.

[16] Junkins, J. L., and Turner, J. D., *Optimal Spacecraft Rotational Maneuvers*, Elsevier, New York, 1986.

[17] Tenne, D., and Singh, T., "The Higher Order Unscented Filter," *Proceedings of the 2003 American Control Conference*, Vol. 3, Inst. of Electrical and Electronics Engineers, Piscataway, NJ, June 2003, pp. 2441–2446.

[18] Wan, E., and van der Merwe, R., "The Unscented Kalman Filter," *Kalman Filtering and Neural Networks*, Wiley, New York, 2001, Chap. 7.

[19] Shuster, M. D., and Oh, S. D., "Three-Axis Attitude Determination from Vector Observations," *Journal of Guidance, Control, and Dynamics*, Vol. 4, No. 1, 1981, pp. 70–77.

[20] Bar-Itzhack, I. Y., Deutschmann, J., and Markley, F. L., "Quaternion Normalization in Additive EKF for Spacecraft Attitude Determination," AIAA Guidance, Navigation, and Control Conference, New Orleans, LA, AIAA Paper 1991-2706 , Aug. 1991.